NREL/TP-254-4593 • UC Category: 233 • DE92001186

Uncertainty of Calorimeter Measurements At NREL's High Flux Solar Furnace

Carl E. Bingham

Prepared for the ASME International Solar Energy Conference, Maui, Hawaii, April 4-8, 1992

National Renewable Energy Laboratory
(formerly the Solar Energy Research Institute)
1617 Cole Boulevard
Golden, Colorado 80401-3393
A Division of Midwest Research Institute
Operated for the U.S. Department of Energy
under Contract No. DE-AC02-83CH10093

December 1991

On September 16, 1991, the Solar Energy Research Institute was designated a national laboratory, and its name was changed to the National Renewable Energy Laboratory.

NOTICE

Printed in the United States of America
Available from:
National Technical Information Service
U.S. Department of Commerce
5285 Port Royal Road
Springfield, VA 22161

Price: Microfiche A01
Printed Copy A02

Codes are used for pricing all publications. The code is determined by the number of pages in the publication. Information pertaining to the pricing codes can be found in the current issue of the following publications which are generally available in most libraries: *Energy Research Abstracts (ERA)*; *Government Reports Announcements* and Index (*GRA* and I); *Scientific and Technical Abstract Reports (STAR)*; and publication NTIS-PR-360 available from NTIS at the above address.

UNCERTAINTY OF CALORIMETER MEASUREMENTS AT NREL's HIGH FLUX SOLAR FURNACE

Carl E. Bingham
National Renewable Energy Laboratory
1617 Cole Blvd.
Golden, CO 80401

ABSTRACT

The uncertainties of the calorimeter and concentration measurements at the High Flux Solar Furnace (HFSF) at the National Renewable Energy Laboratory (NREL) are discussed. Two calorimeter types have been used to date. One is an array of seven commercially available circular foil calorimeters (gardon or heat flux gages) for primary concentrator peak flux (up to 250 W/cm^2). The second is a cold-water calorimeter designed and built by the University of Chicago to measure the average exit power of the reflective compound parabolic secondary concentrator used at the HFSF (over 3.3 kW across a 1.6-cm^2 exit aperture, corresponding to a flux of about 2 kW/cm^2).

This paper discusses the uncertainties of the calorimeter and pyrheliometer measurements and resulting concentration calculations. The measurement uncertainty analysis is performed according to the ASME/ANSI standard PTC 19.1 (1985). Random and bias errors for each portion of the measurement are analyzed. The results show that as either the power or the flux is reduced, the uncertainties increase.

Another calorimeter is being designed for a new, refractive secondary which will use a refractive material to produce a higher average flux (5 kW/cm^2) than the reflective secondary. The new calorimeter will use a time derivative of the fluid temperature as a key measurement of the average power out of the secondary. A description of this calorimeter and test procedure is also presented, along with a pre-test estimate of major sources of uncertainty.

NOMENCLATURE

A	=	cross-sectional exit area of refractive secondary (m^2)
B( )	=	bias error component of measurement or value
C	=	concentration produced by the solar furnace using primary and/or secondary concentrator (flux ratio)
C_p	=	specific heat of water for reflective secondary test (J/kg-deg C)
C_{po}	=	heat capacity of oil for refractive secondary test (J/deg C)
D_e	=	secondary exit diameter (m)
$(dT/dt)_{htr}$	=	rate of temperature rise of oil in refractive secondary calorimeter due to electrical input (deg C/s)
$(dT/dt)_{sun}$	=	rate of temperature rise of oil in refractive secondary calorimeter due to solar input (deg C/s)
$(dT/dt)_{test}$	=	rate of temperature rise of oil in refractive secondary calorimeter due to thermal test input (deg C/s)
h	=	convective heat transfer coefficient between oil and secondary (W/m^2-deg C)
Q	=	average optical power out of refractive secondary (W)
Q_{ch}	=	convective heat transferred from oil to refractive secondary in heater test (W)
Q_{cs}	=	convective heat transferred from refractive secondary to oil in solar test (W)
Q_h	=	electrical power to lamp in reflective secondary calorimeter (W)
Q_{htr}	=	electrical power to refractive secondary calorimeter heater (W)
Q_i	=	average power into reflective secondary cold water calorimeter (W)
Q_{loss}	=	heat lost from secondary calorimeter to ambient air (W)
q_a	=	absorbed flux on circular foil calorimeter (W/m^2)
q_i	=	incident peak flux on circular foil calorimeter (W/m^2)
q_s	=	incident solar radiation as measured by normal incidence pyrheliometer (NIP) (W/m^2)
R( )	=	random error component of measurement or value
ρ	=	density of water (kg/l)
T_{oil}	=	average oil temperature for refractive secondary test (deg C)
T_{sec}	=	secondary temperature for refractive secondary test (deg C)
t	=	students' t distribution for random portion of uncertainty
t_f	=	final time of test for refractive secondary (s)
t_i	=	initial time of test for refractive secondary (s)
U_{95}( )	=	uncertainty (95% coverage) of result
vdot	=	water flow through reflective secondary cold water calorimeter (l/s)
δT	=	temperature rise across cold water calorimeter (deg C)
ε	=	emissivity of circular foil calorimeter (ratio)

INTRODUCTION

NREL's High Flux Solar Furnace

NREL's High Flux Solar Furnace (HFSF) has a unique 30-degree off-axis design (Lewandowski 1989) and a high focal length to diameter ratio of 1.85 that allow it to utilize the non-imaging secondary concentrators developed by the University of Chicago (Gleckman, et al. 1989). With the use of a water calorimeter described later, flux concentrations of 20,000 suns over a 14-mm diameter exit aperture have been obtained with the reflective secondary placed at the focal point of the primary concentrator (Lewandowski, et al. 1991; O'Gallagher, et al. 1991). Concentrations of 50,000 suns are expected with the refractive secondary. Nominal concentration with the multifaceted primary concentrator is about 2300 suns (Bingham and Lewandowski 1991). In this paper, the primary or secondary concentration shall refer to the concentration of the entire solar furnace system, i.e., the ratio of the flux achieved with a particular concentrator(s) (which includes reflection losses from the heliostat) compared to the ambient solar irradiance. An attenuator is used to adjust either the amount of flux or power at the focal point, and a shutter may be used to initiate and terminate flux rapidly.

Primary Concentrator Calorimeter

The instrumentation used to calculate the peak flux and concentration obtained with the multifaceted primary concentrator includes circular foil calorimeters, a normal incidence pyrheliometer (NIP), and a voltmeter. The first step in measurement uncertainty analysis is to define the true values and their governing equations. The incident flux is the absorbed flux as measured by the circular foil calorimeter at the focal point of the primary divided by the emissivity of the calorimeter (measured during calibration by a reflectometer):

$$q_i = q_a / \varepsilon \quad (1)$$

The concentration of the primary concentrator is simply the ratio of the peak incident flux at the focal point, as calculated above, and the solar irradiance, measured by the NIP:

$$C = q_i / q_s \quad (2)$$

Reflective Secondary Calorimeter

The reflective secondary concentrator and the calorimeter shown in Figure 1 were designed and built by the University of Chicago. The secondary concentrator is placed at the focal point of the primary concentrator to further enhance the concentration of solar radiation. The instrumentation used for measurements from which to calculate the average power and concentration obtained with the reflective secondary concentrator includes a water calorimeter, a turbine flowmeter, a frequency-to-voltage converter / indicator, two type-K thermocouples wired as a differential thermocouple (or thermopile), an NIP, a voltmeter, a wattmeter, and a dial caliper to measure the exit diameter of the secondary.

The steady-state average power absorbed by the calorimeter from the reflective secondary can be measured as

$$Q_i = \text{vdot} * \rho * C_p * \delta T + Q_{loss} \quad (3)$$

where Q_{loss} is the portion of the energy absorbed by the secondary calorimeter that is lost to the ambient air by re-radiation and convection. The concentration obtained with the reflective secondary is defined as

$$C = (Q_i / (\pi * (D_e/2)^2) / q_s \quad (4)$$

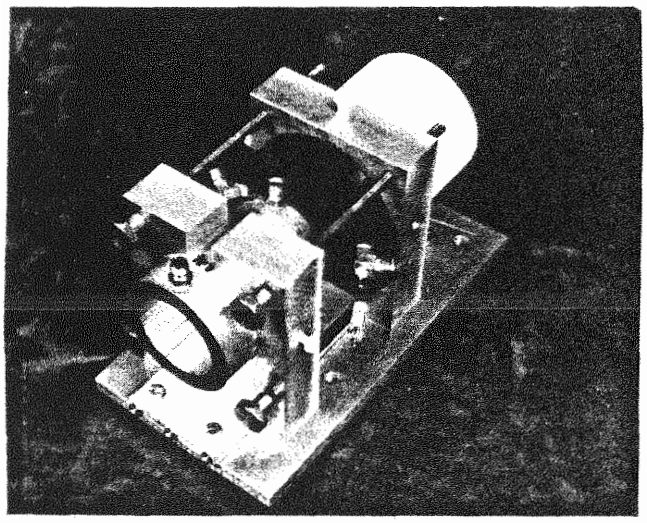

Figure 1. The reflective secondary and calorimeter.

The test procedure is to first perform an end-to-end calibration check of the total system by using a 1-kW lamp inserted into the water calorimeter and comparing the electrical power as indicated by a wattmeter with the thermal power as calculated above. These tests were conducted with great care as to insulation (to avoid heat leaks to ambient) and equilibrium (heat input, flow rate, and temperature difference). It is assumed for the purpose of this analysis that all the electrical power to the lamp was transferred to thermal power, and all the thermal power was transferred to the water ($Q_h = Q_i$). When these tests were conducted, the measurements of electrical power and thermal power agreed to within ±1%.

For the on-sun tests, the reflective secondary and calorimeter were placed at the focal point of the HFSF. With the shutter closed, instrumentation was monitored (especially the temperature rise across the secondary) to verify the system was at equilibrium. The room temperature was monitored to determine any heat loss/gain from the ambient air (Q_{loss}). If a 5 deg C difference existed between the calorimeter water and the room air, Q_{loss} would be about 6 W or 0.2% of the 3.3 kW into the calorimeter. This assumes the calorimeter is covered with 2.5 cm of fiberglass insulation, and a simple UA calculation. Q_{loss} is assumed to be negligible for the purposes of this uncertainty analysis, but typically, as the cooling water heats up, there is a loss from the calorimeter that would increase the calculated power and concentration values. This would be a small positive systematic error.

After equilibrium is reached, the shutter is opened to initiate on-sun testing, and the system is allowed to equilibrate again. Data are then collected for several minutes before closing the shutter. With no solar radiation, the water in the calorimeter cools down to the point that the temperature difference is small (< 0.1 deg C).

Refractive Secondary Calorimeter

The ballistic calorimeter shown in Figure 2 is similar to but larger than those used for previous tests at the University of Chicago (Gleckman 1988). The calorimeter consists of a 12-cm-diameter dewer 17 cm high with a window on the front that is optically coupled to the secondary. It is filled with an oil with an index of refraction matched to that of the secondary and uses a magnetic stirrer to reduce temperature stratification in the oil. Four shielded thermocouples in the oil are used to measure the rate of temperature rise (dT/dt). One thermocouple, located out of the flux, is attached to the secondary to estimate convection between the oil in the calorimeter and the secondary. A 1.5-kW heater immersed in the calorimeter is used for calibration. The 1.5-kW heater is the same range as the 1.3-kW solar input. For either solar or electrical energy input, the temperature rise, dT/dt, is proportional to the energy input. It is assumed that the calorimeter will react to the solar input in a manner similar to the electrical heater to eliminate effects such as changes in fluid properties with temperature.

The details of the measurement and calculations are similar to those included in Gleckman (1988). The test is run as follows: A baseline condition with no energy input is obtained where all four thermocouples should indicate the same temperature in the stirred fluid. In the solar test, a shutter is used to expose the secondary and calorimeter to the sun for an established period. All temperatures measured with the four thermocouples should rise at the same rate, even though their temperatures may not agree. After the prescribed period, the shutter will be closed, and the temperatures should converge. The window thermocouple will enable the convective heat transferred from the secondary to the fluid to be estimated from their temperature difference (T_{sec}-T_{oil}), which is subtracted from the total power to get the radiative input. The calculations are detailed below.

The heater test is run in a similar manner, but electrical energy is substituted for solar energy. The heater test is initiated by supplying power to the electrical heater in the calorimeter, causing the temperature

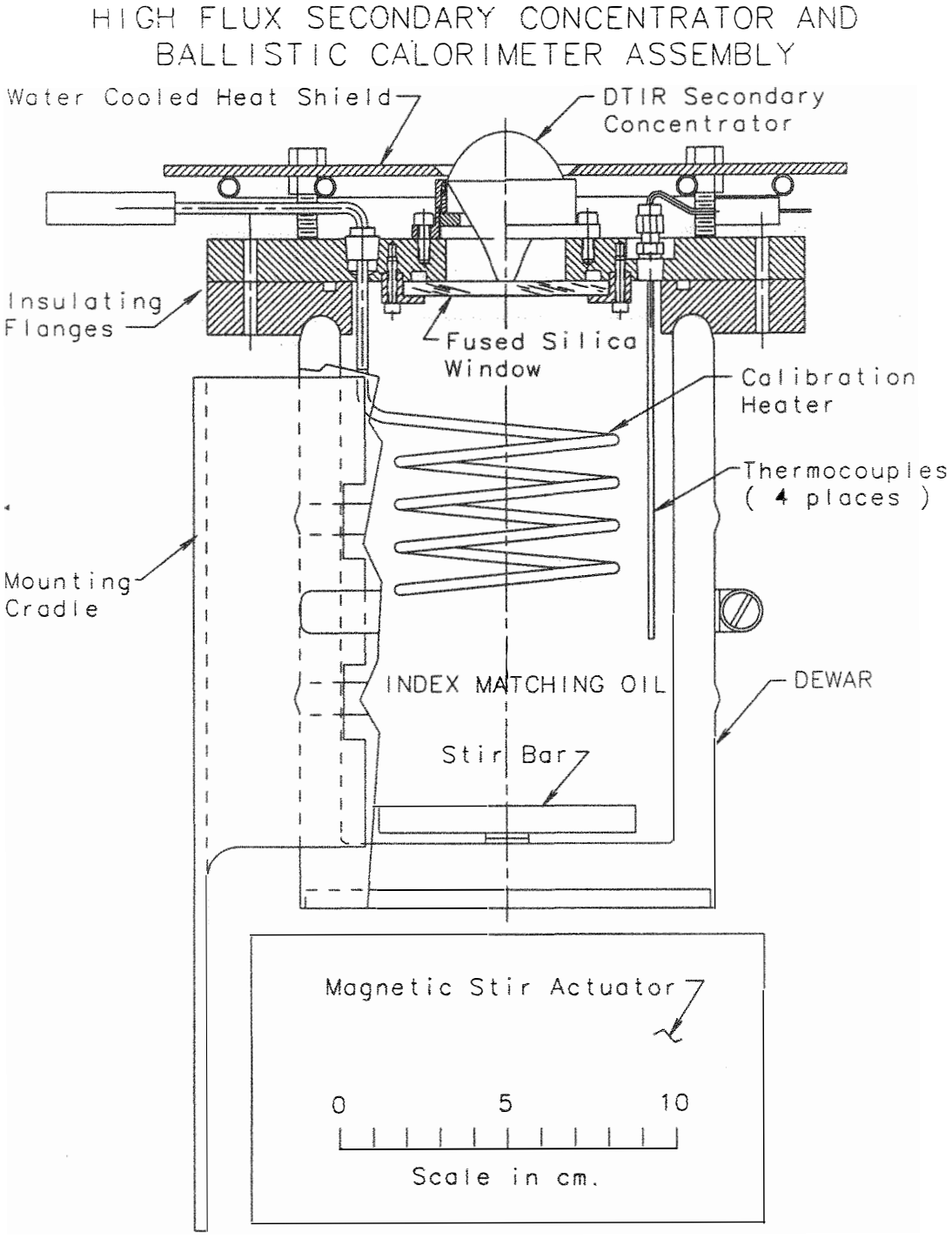

Figure 2. Schematic of refractive secondary and calorimeter (not all thermocouples are shown).

of the oil to rise. After the heater is turned off, the oil cools, and the thermocouples reach the same temperature. The rate of change of temperature due to the electrical energy input is measured during both of these stages: heat-up and cool-down. The rates of change of the two temperatures for the solar and electrical heater tests are then compared.

The average radiative power out of the refractive secondary may be determined according to Gleckman (1988) as follows:

$$Q = [(dT/dt)_{sun} / (dT/dt)_{htr}] * (Q_{htr} - Q_{ch}) - Q_{cs} \quad (5)$$

There are two additional terms; the energy lost from the calorimeter to ambient and the energy gained from the stir bar. However, for the purposes of this analysis, it is assumed that the calorimeter is sufficiently insulated from the surroundings to neglect the loss term. Indeed, typically, the calorimeter will be warmer than the surroundings, and the heat lost would be credited to the calorimeter. The energy transferred into the calorimeter by the stir bar is also neglected in this analysis.

Q_{ch} and Q_{cs}, the convective heat transferred from and to the oil for the heater and solar tests, respectively, can be determined using the heat transfer coefficient, h; for example,

$$Q_{ch} = (h * A/(t_i - t_i)) * \int_{t_i}^{t_f} (T_{sec} - T_{oil})dt \quad (6)$$

The heat transfer coefficient between the secondary and the oil must be determined to calculate Q_{ch} and Q_{cs}. This is done in a separate heat transfer test with a thermal test input to the secondary (Gleckman used a soldering iron), measuring the temperature difference between the secondary and the oil and the cross-sectional area of the secondary. Assuming the fluid is fully mixed, the value of h can be solved from the relation

$$h * A * (T_{sec} - T_{oil}) = C_{po} * (dT/dt)_{test} \quad (7)$$

To evaluate equation 7, the heat capacity of the oil, C_{po}, must be calculated from the electrical heater test data by

$$C_{po} = Q_{htr} / (dT/dt)_{htr} \quad (8)$$

These measurements (for equations 7 and 8) should be done repeatedly (20-30 times) to determine random error. The estimation of the random variation of the heat transfer coefficient h is done in this way and is included in the analysis. In this pre-test analysis, we assume a ±10% random variation.

In summary, we use the heater test data to calculate C_{po}, which is used in the calculation of h from the heat transfer test. The value of h is used to calculate the convective heat transferred between the secondary and the oil in the solar test (Q_{cs} transferred from the secondary to the oil) and the heater test (Q_{ch} transferred from the oil to the secondary). These values may be used to determine the optical power using equation 5.

MEASUREMENT UNCERTAINTY ANALYSIS

To perform a measurement uncertainty analysis of the various calorimeter measurements, the next task is to make up a table of elemental errors, separated into random and bias elements, then estimate the error for each source based on available data. When data are not available, an appropriately conservative engineering estimate may be used. Appendix 1 contains the elemental errors for the primary and reflective secondary flux, power, and concentration measurements.

Bias and Random Error for Each Measurement

The bias and random errors are calculated separately by taking the root-sum-square of each of the elemental errors involved in the measurement. In the present case, this is done for the following measurements:

Primary Flux Measurement
- absorbed heat flux by the circular foil calorimeter
- emissivity of the circular foil calorimeter from reflectometer

Reflective Secondary Power
- flowrate through calorimeter from flowmeter and indicator
- temperature difference across secondary from differential thermocouple
- specific heat and density of water (approximate)
- power measured by wattmeter for reflective secondary

Refractive Secondary Power
- rate of temperature rise for refractive secondary
- electrical power to heater for refractive secondary
- cross-sectional area of refractive secondary
- temperature of oil and refractive secondary

Concentration
- exit diameter of secondary from caliper measurements
- solar radiation measured by the NIP

These values are presented in Table 1.

Sensitivity Analysis

The next step is to determine how sensitive each measurement is to the overall calculation. This may be done by computer perturbation of each measurement parameter or by the partial differentiation of the governing equations with respect to each measurement. The random and bias uncertainties for each measurement are calculated by root-sum-squaring the partial derivatives or sensitivity coefficients, as in the following example:

Random error of incident flux on circular foil calorimeter:

$$R(q_i) = [\ (\delta(q_i) / \delta(q_a))^2 * R(q_a)^2 + (\delta(q_i) / \delta(\varepsilon))^2 * R(\varepsilon)^2\ ]^{1/2} \quad (9)$$

When the calculated random and bias errors and nominal values are substituted into the equations, the random and bias errors for the incident flux, power, and concentration are observed as given in Table 2.

Uncertainty of Incident Flux, Power, and Concentration

The last step is to combine the random and bias errors into the final uncertainty. This is done by taking the root-sum-square of the bias error and the students' t distribution times the random error, for example:

$$U_{95}(Q_i) = \pm[(B(Q_i))^2 + (t * R(Q_i))^2]^{1/2} \quad (10)$$

This value indicates that 95% of the time, the true value of the result should lie within the bounds of $\pm U_{95}$. Therefore, the final results are as presented in Table 3.

The effect of non-nominal flux values was also explored. The analysis was performed at lower levels of solar irradiance and flux to see their effects upon the uncertainty. The attenuator may be used to adjust the amount of flux or power at the focal point. For the primary concentrator, the uncertainty of the concentration and incident flux was similar for levels of solar radiation from 500-1000 W/m^2. For flux levels attenuated to 95% of nominal, the uncertainty of the incident flux and concentration increased from about ±4% to ±6%. The results are plotted in Figure 3.

Table 1. Measurement Bias and Random Errors

Measurement Nominal Value	Random Error	Bias Error
Primary Concentrator Flux		
Absorbed flux		
q_a = 2162 kW/m^2	R(q_a) = ±1.0%	B(q_a) = ±2.0%
Emissivity		
ε = 0.94	R(ε) = ±0.5%	B(ε) = ±2.0%
Reflective Secondary Power		
Flow rate		
vdot = 80 ml/s	R(vdot) = ±0.2%	B(vdot) = ±1.0%
Temperature difference		
δT = 10 deg C	R(δT) = ±1.6%	B(δT) = ±2.1%
Specific heat of H_2O		
C_p = 4180J/kg-deg C	R(C_p) = 0%	B(C_p) = ±0.5%
Density of H_2O		
ρ = 1.0 kg/l	R(ρ) = 0%	B(ρ) = ±0.1%
Wattmeter		
Q_h = 1000 W	R(Q_h) = ±0.1%	B(Q_h) = ±0.5%
Refractive Secondary Power		
Rate of temperature rise		
(dT/dt) = .2 deg C/s	R(dT/dt) = ±0.1%	B(dT/dt) = ±2%
Power to heater		
Q_{htr} = 1100 W	R(Q_{htr}) = ±0.1%	B(Q_{htr}) = ±1%
Cross-sectional area of secondary exit		
A = 24 mm^2	R(A) = ±1%	B(A) = ±1%
Oil temperature		
T_{oil} = 70 deg C	R(T_{oil}) = ±1%	B(T_{oil}) = ±1%
Secondary temperature		
T_{sec} = 50 deg C	R(T_{sec}) = ±1%	B(T_{sec}) = ±1%
Solar radiation		
q_s = 1000 W/m^2	R(q_s) = ±0.5%	B(q_s) = ±1.6%
Reflective secondary exit diameter		
D_e = 14.36 mm	R(D_e) = ±0.2%	B(D_e) = ±0.3%
Refractive secondary exit diameter		
D_e = 5.5 mm	R(D_e) = ±0.2%	B(D_e)= ±0.3%

Table 2. Random and Bias Errors for Power, Concentration, and Wattmeter

Result Nominal Value	Random Error	Bias Error
Primary Concentrator		
Incident flux		
q_i = 2300 kW/m^2	R(q_i) = ±1.1%	B(q_i) = ±2.8%
Concentration		
C = 2300	R(C) = ±1.2%	B(C) = ±3.2%
Reflective Secondary Concentrator		
Power		
Q_i = 4.0 kW	R(Q_i) = ±1.6%	B(Q_i) = ±2.4%
Concentration		
C = 20,600	R(C) = ±1.7%	B(C) = ±2.9%
Water Calorimeter Calibration Check		
Power		
Q_i = 1.0 kW	R(Q_i) = ±3.9%	B(Q_i) = ±5.4%
Wattmeter		
Q_h = 1.0 kW	R(Q_h) = ±0.1%	B(Q_h) = ±0.5%
Refractive Secondary Concentrator		
Power		
Q = 1300 W	R(Q) = ±1.3%	B(Q) = ±3.7%
Concentration		
C = 55,000	R(C) = ±1.6%	B(C) = ±5.0%

Table 3. Final Uncertainty Results

Result	U_{95} Uncertainty	Percent of Nominal Value
Primary incident flux	± 83 kW/m²	± 3.6%
Primary concentration	± 93	± 4.1%
Reflective secondary power	± 0.132 kW	± 4.0%
Reflective sec. concentration	± 928 suns	± 4.5%
Reflective sec. wattmeter	± 0.056 kW	± 0.6%
Refractive secondary power	± 59 W	± 4.5%
Refractive sec. concentration	± 3300	± 6.0%

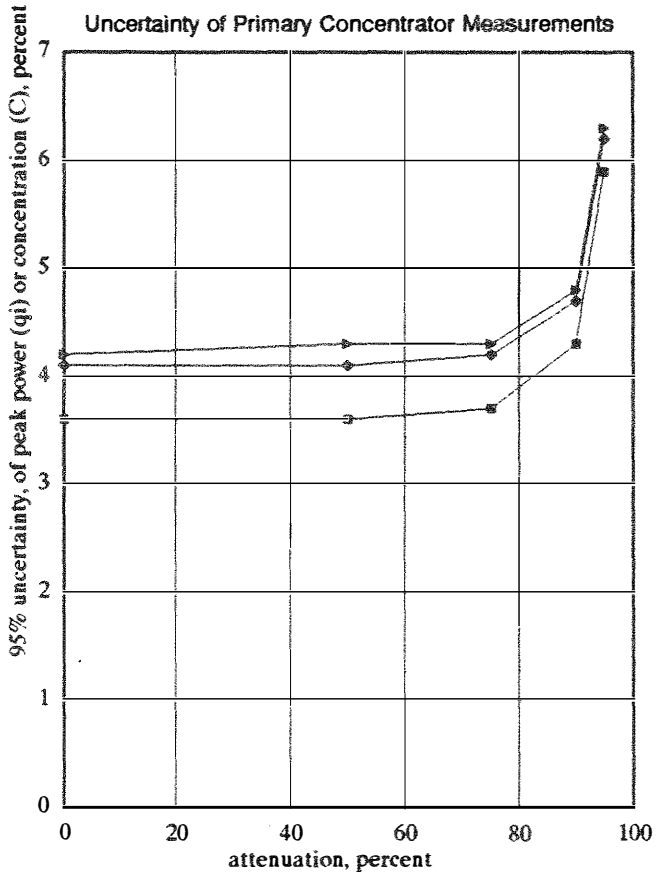

Figure 3. Variation of uncertainty of primary concentrator measurements with attenuation and solar irradiance. Note that $U_{95}(q_i)$ is not sensitive to solar irradiance.

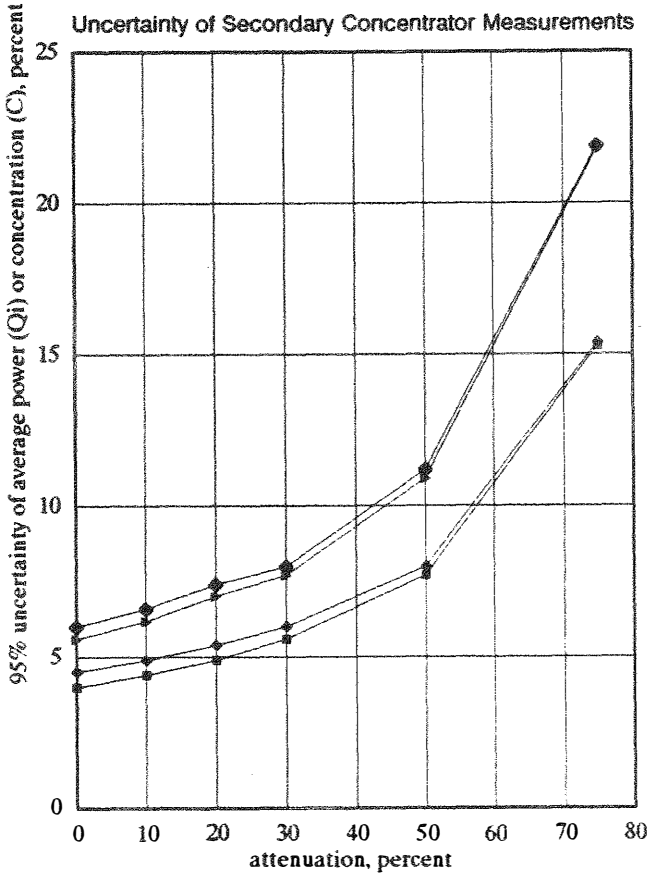

Figure 4. Variation of uncertainty of reflective CPC secondary concentrator measurements with attenuation and solar irradiance.

For the reflective secondary concentrator, Figure 4 shows the relationship between attenuation, insolation, and uncertainty in power and concentration. If the solar radiation drops to 700 W/m^2, the uncertainties of the power and concentration rise to ±5.6% and ±6.0%, respectively. Similar results occur for lower power that would result from attenuation. For operation with 30% attenuation at 700 W/m^2, the uncertainty of the power and concentration would both be around ±8%, which would be similar to 50% attenuation at full sun. The uncertainties are the same because they are both driven by the temperature difference across the water calorimeter, which at an equal flow are reduced to 49% and 50%, respectively.

The uncertainties of the refractive secondary power and concentration at nominal values are estimated to be ±4.5% and ±6%, respectively. The pre-test results from the refractive secondary measurement uncertainty analysis indicate that the critical measurement is the rate of temperature rise of the oil in the secondary for not only the solar and heater tests, but also the heat transfer test to calculate h. It is estimated that the measurements of time and temperature can be made such that the rate of temperature rise can be calculated to a ±2% accuracy. The most difficult

measurement is the evaluation of h, which, in previous tests, had a random variation of ±10%. However, the ±10% variation affects the final value of Q and C by less than 1%.

Potential for Reduction of Uncertainties

For the primary concentrator measurements, there is little that can be done to reduce the uncertainties of flux and concentration significantly. To reduce the uncertainties of the power and concentration of the reflective secondary significantly, the temperature difference measurement must be addressed. By reducing the temperature uncertainty from ±3.8% for the reflective secondary on-sun power to ±1.7%, the overall uncertainty of the power measurement can be reduced from ±4.0% to ±2.5%. This would also reduce the uncertainty of the concentration measurement from ±4.5% to ±3.3%.

There are two ways to reduce the temperature difference uncertainty. One is to change from a thermocouple to a sensor with more sensitivity, such as an RTD or thermistor. Another approach would be to decrease the flow rate, thus increasing the temperature difference across the water calorimeter. Assuming the difficulty in measuring lower flow rates is with the meter and not elsewhere, this could be done by using a flowmeter with a lower range. If it were possible to reduce the flow from 60 ml/s to 30 ml/s, increasing the temperature difference from 4 deg C to 8 deg C, the uncertainty of the power measurement of the water calorimeter with the lamp could be reduced from ±9.5% to ±4.9%.

For the refractive secondary calorimeter, reducing the ±2% uncertainty of the rate of temperature rise to ±1% would reduce the uncertainty of the power and concentration measurements from ±4.5% and ±6% to ±3% and ±5%, respectively. This might be done using more accurate temperature sensors, such as RTDs.

CONCLUSIONS

For the primary concentrator, the uncertainty of the incident peak flux measurements by the circular foil calorimeters is ±3.6% at full power and levels of solar irradiation between 500-1000 W/m^2. At 10% and 5% flux (concentrations of 230 and 115 suns, respectively), this value increases to ±4.3% and ±5.9%, respectively. The uncertainty of the concentration is ±4.1% on a sunny day at flux levels between 25% and 100%, representing concentrations of 575-2300 suns. At lower flux levels of 10% and 5%, the concentration uncertainty increases to ±4.8 and ±6.3%, respectively.

For the reflective secondary tests, the uncertainty of the secondary exit average power measurements by the water calorimeter is ±4.0% at maximum flux and a solar irradiation level of 1000 W/m^2. The uncertainty of the secondary concentration is ±4.5% on a sunny day. If the solar direct beam, as measured by the NIP drops to 700 W/m^2, the uncertainties of the power and concentration rise to ±5.6% and ±6.0%, respectively. Similar results occur for lower flux levels that would result from attenuation. If we operated with 30% attenuation at full sun, the uncertainty of the power and concentration would be the same, ±5.6% and ±6.1%, respectively.

For the calibration check of the water calorimeter, the uncertainty of the average power measurement with the water calorimeter is ±9.5% at 1 kW and with the wattmeter ±0.6% at 1 kW. This indicates the relative uncertainty of the wattmeter is sufficient to check the water calorimeter. During testing, these two values agreed to within ±1%. The higher uncertainty for the water calorimeter measurement is primarily due to the lower temperature difference at 1 kW.

For the reflective secondary, the most critical measurement is the temperature difference across the calorimeter. In order to reduce this uncertainty, a more accurate temperature sensor would be needed and/or a flowmeter with a lower range in order to significantly increase the temperature difference.

For the refractive secondary, the pre-test measurement uncertainty analysis shows that an overall measurement uncertainty for average power and concentration is estimated to be within ±4.5% and ±6%, respectively. The most critical measurement in this test is the rate of temperature rise in all three tests: solar, heater, and heat transfer. The uncertainties are also expected to increase as the power level is decreased, much like the measurements for the primary and reflective secondary.

ACKNOWLEDGEMENTS

This work was supported by the Solar Industrial Program of the U.S. Department of Energy.

REFERENCES

ASME/ANSI, PTC 19.1, 1985, *Measurement Uncertainty*. Supplement to ASME Performance Test Codes, ASME NY, NY, 1986.

Bingham, C., and Lewandowski, A., 1991, "Capabilities of SERI's High Flux Solar Furnace," *Proceedings of the 1991 ASME/JSME/JSES International Solar Energy Conference*, pp. 541-545.

Gleckman, P., 1988, "Achievement of Ultrahigh Solar Concentration with Potential for Efficient Laser Pumping," *Applied Optics*, Vol. 27, No. 21, p. 4385.

Gleckman, P., O'Gallagher, J., and Winston, R., 1989, "Concentration of Sunlight to Solar-Surface Levels Using Non-Imaging Optics," *Nature*, Vol. 339, pp. 198-200.

Lewandowski, A., 1989, "The Design of an Ultra-High Flux Solar Test Capability," *Proceedings of the Intersociety Energy Conversion Engineering Conference IECEC-89*, Washington, DC.

Lewandowski, A., Bingham, C., O'Gallagher, J., Winston, R., and Sagie, D., 1991, "One- and Two-Stage Flux Measurements at the SERI High Flux Solar Furnace," *Proceedings of the 1991 ASME/JSME/JSES International Solar Energy Conference*, pp. 329-335.

Myers, D., 1988, "Uncertainty Analysis for Thermopile Pyrometer and Pyrheliometer Calibrations Performed by SERI," Technical Report TR-215-3294, National Renewable Energy Laboratory, Golden, CO.

O'Gallagher, J., Winston, R., Zmola, C., Benedict, L., Sagie, D., and Lewandowski, A., 1991, "Attainment of High Flux-High Power Concentration Using a CPC Secondary and the Long Focal Length SERI Solar Furnace," *Proceedings of the 1991 ASME/JSME/JSES International Solar Energy Conference*, pp. 337-343.

APPENDIX 1. ELEMENTAL ERRORS

Error	Random	Bias	[Source]
Calibration			
Voltmeter(μv)	±3	±0	[1]
NIP (μv/W/m^2)	±0.032	±0.1413	[2]
Circ Foil Calrmtr (μv/kW/m^2)	±0.034	±0.0680	[1]
Emissivity (ratio)	±0.005	±0.02	[3]
Flowmeter (kg/s)	±0.05%	±0.5%	[1]
Flow indicator (kg/s)	±0.04%	±0.66%	[4]
Differential TC (deg C)	±0.058	±0.040	[4]
Wattmeter (W)	±0.01%	±0.1%	[4]
Calipers (mm)	±0.1%	±0.2%	[5]
Acquisition			
Voltmeter(μv)	±3	±2	[1]
NIP (W/m^2)	±0.35%	±0.03% CF	[2]
Circ Foil Calrmtr (kW/m^2)	±0.1%	±0.04% CF	[1]
Flowmeter (kg/s)	±0.1%	±0.5%	[1]
Flow indicator (kg/s)	±0.1%	±0.5%	[6]
Differential TC (deg C)	±0.1	±0.2	[6]
Wattmeter (W)	±0.1%	±0.5%	[6]
Calipers (mm)	±0.17%	±0.2%	[5]
Data Reduction			
Voltmeter(μv)	±0.01%	±0	[6]
NIP (μv/W/m^2)	±0.01% CF	±0.01% CF	[6]
Circ Foil Calrmtr (μv/kW/m^2)	±0.01% CF	±0.01% CF	[6]
Flow indicator (kg/s)	±0.05%	±0.1%	[6]
Differential TC (deg C)	±0.01%	±0.03	[6]
Wattmeter (W)	±0.01%	±0.02%	[6]
Density of water (kg/l)	±0.01%	±0.1%	[6]
C_p of water (W-s/kg-deg C)	±0.01%	±0.5%	[6]
Calipers (mm)	±0.01%	±0.5%	[5]

Sources of estimates:
[1] calibration report and catalog specifications
[2] Myers (1988) and the calibration report for the specific sensor
[3] calibration report and laboratory measurements
[4] NREL calibration data and catalog specifications
[5] multiple measurements of a known standard
[6] conservative engineering estimate

Note: Percentages are of nominal values, except where calibration factors (CF) are noted.